

Rewiring the severe acute respiratory syndrome coronavirus (SARS-CoV) transcription circuit: Engineering a recombination-resistant genome

Boyd Yount*, Rhonda S. Roberts*, Lisa Lindesmith*, and Ralph S. Baric*^{†‡§}

*Department of Epidemiology, Program in Infectious Diseases, School of Public Health, [†]Department of Microbiology and Immunology, School of Medicine, and [‡]Carolina Vaccine Center, University of North Carolina, Chapel Hill, NC 27599

Communicated by Peter Palese, Mount Sinai School of Medicine, New York, NY, June 29, 2006 (received for review May 15, 2006)

Live virus vaccines provide significant protection against many detrimental human and animal diseases, but reversion to virulence by mutation and recombination has reduced appeal. Using severe acute respiratory syndrome coronavirus as a model, we engineered a different transcription regulatory circuit and isolated recombinant viruses. The transcription network allowed for efficient expression of the viral transcripts and proteins, and the recombinant viruses replicated to WT levels. Recombinant genomes were then constructed that contained mixtures of the WT and mutant regulatory circuits, reflecting recombinant viruses that might occur in nature. Although viable viruses could readily be isolated from WT and recombinant genomes containing homogeneous transcription circuits, chimeras that contained mixed regulatory networks were invariably lethal, because viable chimeric viruses were not isolated. Mechanistically, mixed regulatory circuits promoted inefficient subgenomic transcription from inappropriate start sites, resulting in truncated ORFs and effectively minimize viral structural protein expression. Engineering regulatory transcription circuits of intercommunicating alleles successfully introduces genetic traps into a viral genome that are lethal in RNA recombinant progeny viruses.

regulation | systems biology | vaccine design

Live virus vaccines represent a crucial intervention strategy that has been documented to improve the overall health of populations. Concerns regarding reversion to virulence by mutation and recombination, coupled with the associated challenges in developing these vaccines commercially, have diminished the appeal of live virus vaccines (1, 2). The dichotomy between the well known protective efficacy and the costs and risks of developing live virus vaccines has been recognized as a Grand Challenge in Global Health by the National Foundation for Infectious Diseases, which has called for new methods to prevent reversion or recombination repair.

Severe acute respiratory syndrome coronavirus (SARS-CoV) emerged suddenly and spread worldwide in 2003, causing ≈ 800 deaths (3). Zoonotic SARS-CoV strains, common in farm animals and bats, dictate a need for continued surveillance and the development of efficacious vaccines (4, 5). SARS-CoV is a tractable system for innovative live virus vaccine design because the pathogen is highly virulent and replicates efficiently in animal models, and a robust reverse genetic system is available. Importantly, CoVs undergo RNA recombination events at high frequency, and recombination-mediated vaccine failures in animals are a problem (6).

SARS-CoV contains a positive, single-stranded, $\approx 29,700$ -nt RNA genome bound by the nucleocapsid protein (N) and an envelope containing the S, ORF3a, E, and M structural proteins. The SARS-CoV genome contains nine ORFs, and ORF1 encodes the viral replicase proteins that are required for subgenomic and genome-length RNA synthesis (7). Downstream of ORF1 and interspaced among the structural genes are the unique SARS-CoV group-specific genes (ORF3a/b, ORF6,

ORF7a/b, ORF8a/b, and ORF9b) that are not necessary for replication in cell culture (8). ORFs 2–8 are encoded in subgenomic mRNAs (mRNAs 2–9) synthesized as a nested set of 3' coterminal molecules. Leader RNA sequences, encoded at the 5' end of the genome, are joined to body sequences at distinct transcription regulatory sequences (TRSs) that contain the core sequence ACGAAC (7, 9). SARS-CoV likely uses transcription attenuation to synthesize both full- and subgenomic-length negative strand RNAs containing antileader sequences, which then function as the templates for the synthesis of like-sized mRNAs (10, 11). Transcription attenuation is regulated by interactions between a leader TRS (TRS-L) and body TRS (TRS-B) circuit (12). Expression of each subgenomic mRNA requires extensive communication by means of base pairing between the 5' end TRS-L sequence and the appropriate TRS-B sequence. Most studies support a strong role for a core consensus motif of six to eight nucleotides that guide base pairing and duplex formation between nascent negative strands and the TRS-L site at the 5' end of the genome. The interaction is assisted to a lesser extent by surrounding (mostly downstream) sequences (12, 13).

In this report, we introduce a TRS circuit that regulates efficient expression of the SARS-CoV subgenomic mRNAs. Importantly, recombination events with WT virus trigger lethal incompatibilities in the TRS circuitry, restricting the number of viable recombinant viruses. This study provides an example of a successful redesign of the regulatory circuit of a mammalian virus.

Results

TRS Function in SARS-CoV Transcription. To remodel the SARS-CoV TRS circuit, we replaced the nonessential ORF7a/b domain with the *Renilla* luciferase gene under the control of the ORF7a/b TRS-B (icSARS-CoV Luc). We then engineered double (icSARS-CoV Luc1) and triple (icSARS-CoV Luc2) mutations that should specifically disrupt the ORF7a/b TRS-B circuit, theoretically blocking efficient mRNA 7 transcription. The WT SARS-CoV TRS-B (ACGAAC) was replaced with double (TRS-1, ACGGAT) and triple (TRS-2, CCGGAT) mutations, the latter not being encoded elsewhere in the Urbani genome (Fig. 1A). In fact, the remodeled TRS-2 sequence is unique among CoVs.

Consistent with reports describing a SARS Δ ORF7a/b GFP replacement virus (14), icSARS-CoV Luc replicated like WT virus, achieving titers of $> 2 \times 10^7$ pfu/ml within 20 h after

Conflict of interest statement: No conflicts declared.

Freely available online through the PNAS open access option.

Abbreviations: SARS-CoV, severe acute respiratory syndrome coronavirus; TRS, transcription regulatory sequence; TRS-L, leader TRS; TRS-B, body TRS.

[§]To whom correspondence should be addressed at: Department of Epidemiology, School of Public Health, University of North Carolina, 3304 Hooker Research Building, Chapel Hill, NC 27599-7435. E-mail: rbaric@email.unc.edu.

© 2006 by The National Academy of Sciences of the USA

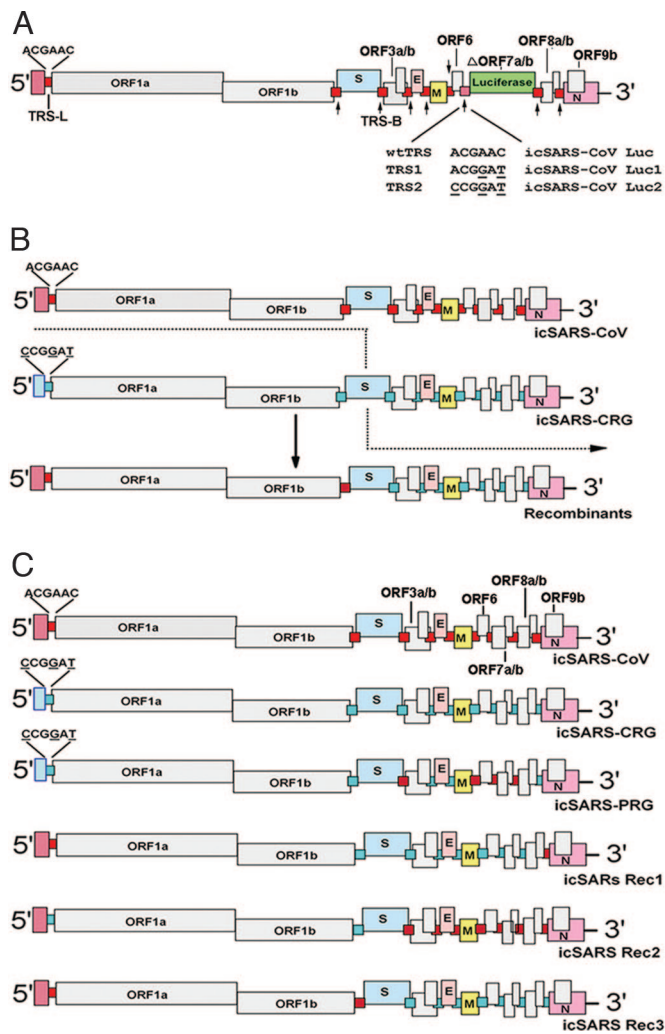


Fig. 1. Genome organization of SARS-CoV recombinant viruses. ORF7a/b of SARS-CoV was replaced with the *Renilla* luciferase gene, resulting in icSARS-CoV Luc. Second- and third-generation constructs were engineered, which contained two or three mutations in the ORF7a/b TRS, altering the ACGAAC to the double (TRS-1, ACGGAT) or triple (TRS-2, CCGGAT) mutant in icSARS-CoV Luc1 and icSARS-CoV Luc2, respectively. The TRS-2 circuit was placed throughout the icSARS-CoV CRG genome or at select sites within the icSARS-CoV PRG genome to allow for structural gene expression. A series of chimeric viruses was assembled by using the icSARS-CoV and icSARS-CoV CRG molecular clones. (A) Genetic organization of the icSARS-CoV luciferase replacement viruses. Red boxes represent WT virus TRS sites. The TRS-B sites are marked by arrows. (B) Organization of the icSARS-CoV CRG and icSARS-CoV PRG recombinant viruses. TRS sites are indicated by small red (icSARS-CoV) or blue (icSARS-CoV CRG) squares, respectively. (C) Genetic organization of chimeric viruses.

infection. In icSARS-CoV Luc-infected cells, *Renilla* luciferase expression peaked at ≈ 5 logs above background (Fig. 2A). Under identical conditions, icSARS-CoV Luc1 and icSARS-CoV Luc2 displayed 1.5- to 2.0-log reductions in luciferase expression. Western blot confirmed the reduction in *Renilla* luciferase, but not N protein expression, after infection (Fig. 2B and C). Northern blot analyses clearly demonstrated the expected size increases in mRNAs 3–7, but not mRNAs 8–9, associated with the replacement of ORF7 with the larger *Renilla* luciferase gene. Concordant with reduced luciferase protein expression, TRS-2 clearly reduced expression of subgenomic mRNA 7 (Fig. 2D).

Rewiring the TRS Transcription Circuit. The entire WT TRS circuit was replaced with the TRS-2 sequence that differed from the

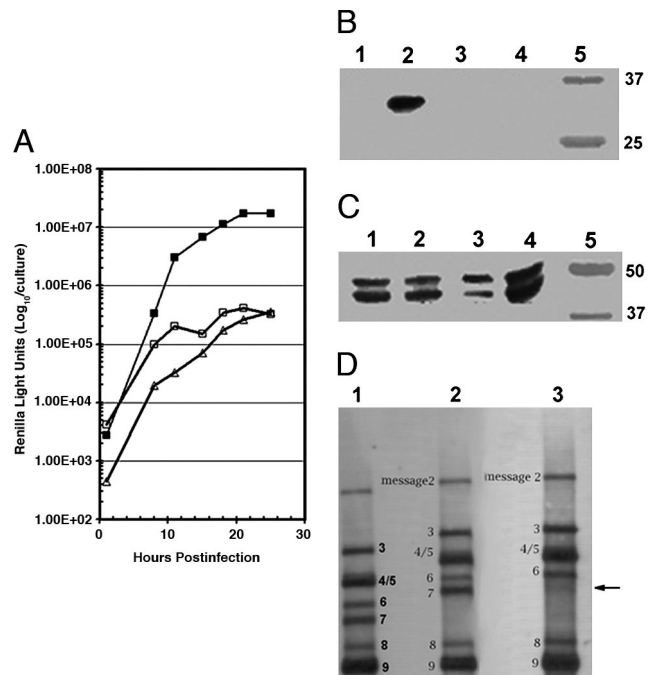


Fig. 2. Phenotype of icSARS-CoV Luc recombinant viruses. Infected cells were lysed at various times after infection. (A) *Renilla* luciferase light units were quantified in triplicate. ■, icSARS-CoV Luc; □, icSARS-CoV Luc1; △, icSARS-CoV Luc2. (B and C) At 12 h after infection, cell lysates were separated on polyacrylamide gels and probed with antisera directed against the *Renilla* luciferase protein (B) or the SARS N protein (C). Lane 1, icSARS-CoV; lane 2, icSARS-CoV Luc; lane 3, icSARS-CoV Luc1; lane 4, icSARS-CoV Luc2. (D) Overall mRNA 7 levels were reduced in icSARS-CoV Luc2-infected cultures. Lane 1, icSARS-CoV; lane 2, icSARS-CoV Luc; lane 3, icSARS-CoV Luc2.

WT TRS sequence at three nucleotide positions to yield the icSARS CRG genome. In addition, a second genome was designed with a scrambled TRS network. The icSARS PRG genome contained an intact TRS-2 regulatory circuit that was designed to specifically promote efficient expression of subgenomic transcripts (mRNAs 2, 4, 5, and 9) encoding the four essential structural proteins, S, E, M, and N, respectively. However, WT TRS-B sites were retained upstream of each of the group-specific genes ORF3a/b, ORF6, ORF7a/b, and ORF8a/b. We hypothesized that inefficient leader–body TRS base pairing should attenuate expression of transcripts encoding the group-specific genes in the icSARS PRG genome (Fig. 1C).

Recombinant virus icSARS CRG and icSARS PRG both replicated efficiently in Vero cells, approaching titers of $\approx 5.0 \times 10^7$ pfu/ml within 20 h after infection, equivalent to WT (Fig. 3A). Growth was slightly delayed after icSARS CRG infection. Northern blot analyses revealed appropriately sized subgenomic mRNA species in icSARS CRG-infected cells, typical of WT SARS-CoV infection (Fig. 3B). Importantly, icSARS PRG infection was characterized by robust mRNA 1, 2, 4, 5, and 9 synthesis but reduced and/or aberrant subgenomic mRNA synthesis driven from the WT TRS-B sites that regulated expression of the group-specific ORFs. For example, expression of mRNAs 3 and 7 was reduced by $\approx 50\%$, mRNA 6 was of incorrect size, and mRNA 8 was not detected. Western blot analyses confirmed abundant levels of the structural proteins S and N in all recombinant and WT viruses, abundant ORF3a in WT and icSARS CRG, but little if any ORF3a in icSARS PRG-infected cultures (Fig. 3C).

Analysis of leader–body TRS junctions in WT icSARS-CoV and icSARS CRG revealed the expected usage of the appropriate WT or mutant TRS site (data not shown). In icSARS PRG,

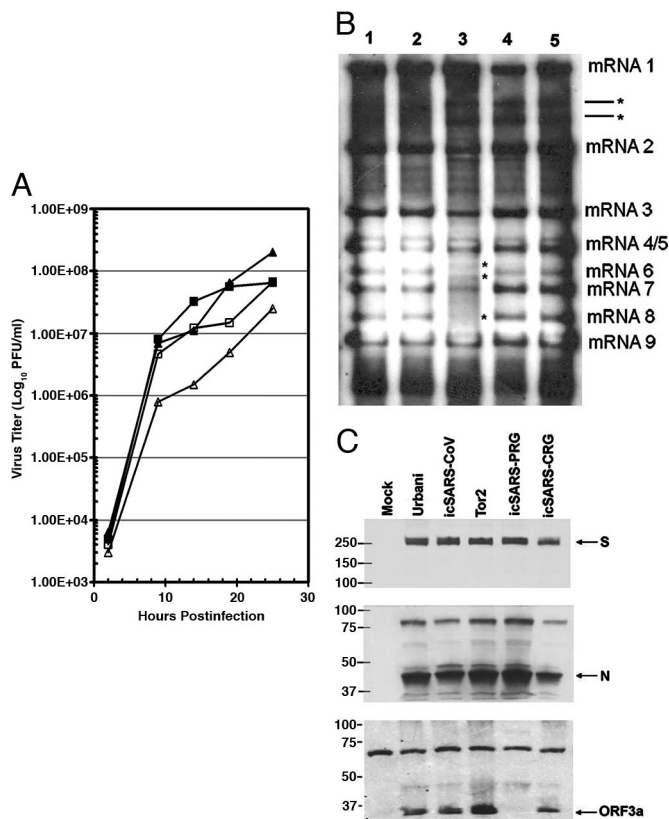


Fig. 3. Phenotypic characterization of SARS-CoV recombinants encoding redesigned TRS networks. The icSARS-CoV CRG and icSARS-CoV PRG were inoculated onto Vero cells at a multiplicity of infection of 0.1. In addition, RNA and protein were harvested at 12 h after infection. (A) Recombinant virus growth in Vero E6 cells. ■, WT Urbani; □, icSARS-CoV; ▲, icSARS-CoV PRG; △, icSARS-CoV CRG no. 2. (B) Northern blot analysis of Urbani. Lane 1, icSARS-CoV; lane 2, icSARS-CoV PRG; lane 3, two different plaque-purified icSARS-CoV CRG virus-infected cells; lane 4, CRG no. 2; lane 5, CRG no. 3. Asterisks mark some transcripts noted in icSARS-CoV PRG- and CRG-infected cells. (C) Western blot analysis evaluating S (Top), N (Middle), or ORF3a (Bottom) expression.

leader-body TRS-2 sites drove expression of subgenomic mRNAs encoding the structural proteins, demonstrating efficient communication between networked leader-body TRS sites. In contrast, the WT TRS site, ACGAAC, was rarely used for initiating expression of the group-specific ORF encoding subgenomic RNAs (data not shown). Most often, downstream noncanonical TRS sites were activated, most likely because they displayed high homology with the leader TRS-2 junction. Aberrant leader-body junction sites in mRNA 3 often encoded N-terminal deletions in the ORF 3a protein (Fig. 4A). The group-specific ORFs were not essential for SARS-CoV growth in culture (8).

Remodeled TRS Circuits Are Lethal in RNA Recombinant Genomes. RNA recombination between WT and icSARS CRG genomes may generate incompatible TRS regulatory circuits (Fig. 1B). To test this hypothesis, a series of WT and chimeric recombinant viruses was engineered (Fig. 1C). Reflecting a double recombinant containing cross-over sites in ORF8 and the replicase ORF, the icSARS Rec1 genome preserves only the WT TRS-L and N gene TRS-B circuit. Reciprocal chimeric genomes were also designed to mimic natural recombinants that would have originated from a single cross-over event within the S gene. Such recombinants would have efficient communication between the WT (icSARS-Rec2) or rewired (icSARS-Rec3) TRS-L and a

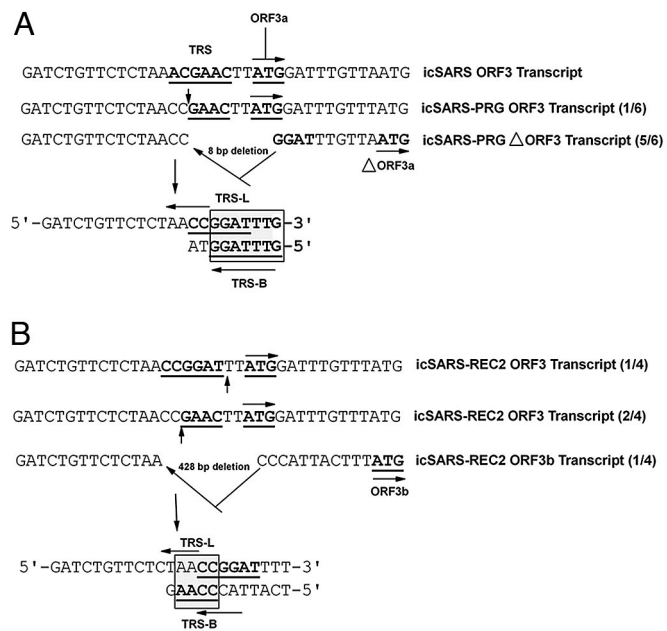


Fig. 4. Structure of icSARS-CoV recombinant virus ORF3a transcripts. Cultures of cells were infected with recombinant viruses. The leader-containing amplicons were purified by gel electrophoresis, subcloned, and then sequenced. (A) Organization of icSARS-CoV PRG ORF3a leader-containing transcripts. (B) ORF3a transcripts expressed in cultures transfected with chimeric recombinant genome no. 2. Cross-over sites are shown in gray boxes, and arrows represent the direction of template switching based on the transcription attenuation model for CoV RNA synthesis. Underlined ATG represents the start codon.

TRS-B site regulating mRNA 2 expression but not the remaining subgenomic mRNAs. Similar recombinants have been noted in mouse hepatitis virus (15).

Full-length icSARS-CoV, icSARS CRG, and the chimeric genomes were electroporated into Vero cells. One-fifth of the cells were used to determine the number of infectious centers (Fig. 5A). The remaining cells were maintained in complete medium. In three separate transfection experiments, >10³ infectious centers were detected for icSARS CRG and icSARS-CoV. Under identical conditions, no infectious centers were detected in icSARS Rec no. 1–3 transfected cultures. Moreover, icSARS-CoV and icSARS CRG virus titers increased from <10 (assay sensitivity) to >10⁷ pfu/ml by 72 h after electroporation. No virus was detected in icSARS-Rec no. 1–3 transfected cultures through 72 h or after three additional serial passages at 48-h intervals (Fig. 5B).

Using RT-PCR, we readily detected leader-containing transcripts in WT and icSARS CRG transfected cultures at 24 h and increasing abundance by 48 h. These leader-containing transcripts originated at the appropriate network of leader-body TRS circuits (not shown). In contrast, only low levels of subgenomic mRNA transcripts were detected in icSARS Rec no. 1–3 transfected cultures at 24 h, most notably in icSARS Rec no. 2. Leader-containing transcripts had almost disappeared by 48 h (Fig. 6A). In chimeric viruses, leader-containing RNAs mostly originated from noncanonical TRS sites located downstream of the appropriate start location (Fig. 4B). In many cases, noncanonical site usage resulted in large N-terminal deletions in critical structural genes such as M, which is essential for the production of infectious progeny virions (Fig. 6B).

Discussion

Genetic recombination is a fundamental evolutionary process, and recombination repair of attenuated vaccines is not uncom-

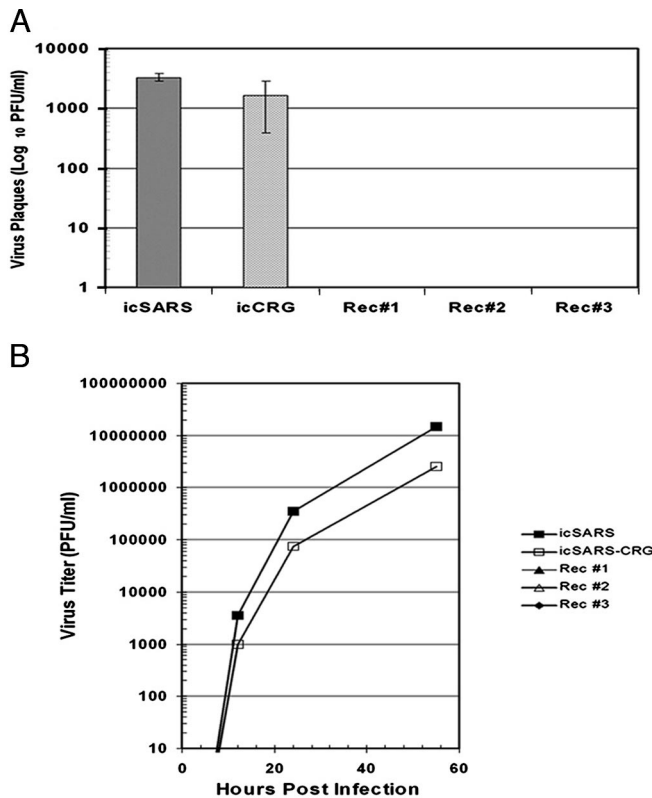


Fig. 5. Infectivity of WT and chimeric recombinant RNAs. Cultures were transfected with RNA transcripts encoding the icSARS-CoV, icSARS-CoV CRG, icSARS-CoV Rec1, icSARS-CoV Rec2, and icSARS-CoV Rec3 genomes. Cells were plated onto monolayers and overlaid with medium containing agarose for determination of infectious centers or placed into 25-cm² flasks. (A) Infectious center assay of recombinant transcripts. (B) Virus titers at different times after transfection. ■, icSARS-CoV; □, icSARS-CoV CRG.

mon (1, 2, 6, 16, 17). RNA recombination occurs when the viral replicase switches from donor to acceptor templates during RNA synthesis, followed by the use of the nascent RNA as a primer for continued RNA synthesis. Replication rates, RNA secondary structure, genome size, the RNA replicase protein complex, and host factors regulate the frequency of RNA recombination events; however, successful inheritance is governed by the relative fitness of the recombinant progeny (18–21). Viable recombinants have been described between different CoV strains and serogroups, including mouse hepatitis virus and SARS-CoV (22). By rewiring the SARS-CoV transcription circuit, we identified a method that specifically reduced the fitness of progeny RNA recombinant viruses.

Empirical studies with a small plant virus suggest that the successful inheritance of a particular genetic fragment is inversely proportional to and constrained by its number of intragenome interactions (23). CoV transcription networks involve complex interactions among the viral replicase complex, cis and transacting sequence motifs, and perhaps host factors. This network probably imparts discrete constraints on the ability of a genome to evolve by recombination. In the 3' end of the mouse hepatitis virus genome, gene order rearrangements reduce the number of recombinant viruses recovered (24). New regulatory circuits have been designed to control the lysogenic and lytic phases of infection in phage (25, 26), and genome order has been remodeled in some phage and mammalian viruses (27, 28). However, complete redesign of a virus transcription circuit has not been reported. We engineered a regulatory circuit into the backbone of a recombinant SARS-CoV that limits the viability

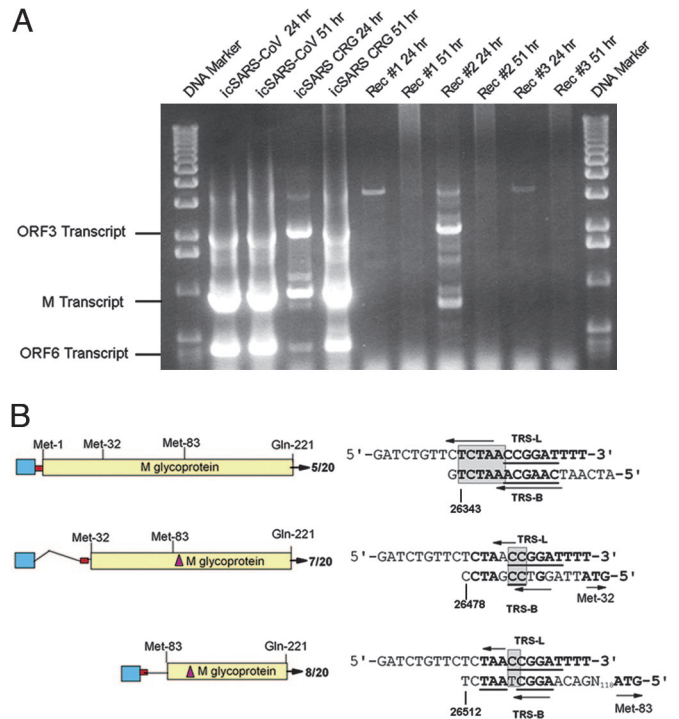


Fig. 6. Leader-body TRS junctions in WT and chimeric recombinant viruses. Intracellular RNA was isolated at 24 and 51 h after transfection. Using leader- and ORF7-specific primer pairs, leader-containing amplicons were separated on agarose gels, excised, subcloned, and sequenced. (A) Leader-containing amplicons in transfected cultures. (B) Leader-body junctions in mRNA 5' transcripts encoding the SARS M glycoprotein. Although the expected leader-body junctions were noted for icSARS-CoV and icSARS-CoV CRG, noncanonical mRNA 5' TRS sites were identified in chimeric viruses. Cross-over site locations are shown by gray boxes, and arrows represent the direction of template switching. Underlining marks the ATG start codon.

of recombinant progeny. These studies not only describe a unique paradigm for studying CoV transcription circuit design, evolution, and function but also allow the engineering of safer nidovirus live virus vaccine chassis.

Among the Coronaviridae, different TRS motifs have been described that function in the regulation of transcription. The engineered TRS CCGGAT circuit is unique and should function poorly after insertion into any other CoV genome. Our data also demonstrate that disruption of a TRS-B site specifically debilitates expression of its specific subgenomic mRNA and that mutations in the TRS-L suppress expression of all subgenomic mRNAs. As with other CoVs, mutations inserted within a SARS-CoV TRS-B site persisted in subgenomic mRNAs, providing further support for the transcription attenuation model (10–12). In chimeric genomes, transcription attenuation was also guided by downstream sequence motifs that could form base pair duplexes with the TRS-L; however, these sites were inefficient and usually mapped within ≈170 nt. Occasionally, leader-containing transcripts originated within flanking sequences adjacent to the core TRS sequence. These data suggest that a 9–12 nt TRS circuit that included some upstream/downstream flanking nucleotides might result in more stable artificial circuits. Interestingly, noncanonical TRS sites that were transcriptionally active in the icSARS PRG genome were silent in the icSARS CRG genome (Fig. 3B). We believe that TRS recognition is hierarchical and based on higher order RNA structure, local RNA structure, replicase function, and TRS-L/TRS-B sequence homology. In the absence of a perfect TRS match, the transcription network selects the next best sequence match in the

proximal locale, but at reduced rates. The exact nature of this transcription network remains largely unexplored.

Chimeric genomes were crippled because incompatible TRS circuitry was less efficient, reducing mRNA synthesis. In the icSARS-CoV Rec no. 2 chimera, nearby noncanonical sites were preferentially engaged in subgenomic transcription. These non-canonical sites were defined by sequences that provided limited base pair duplex formation between negative strands and TRS-L. Among mRNA 5 transcripts, 75% encoded for M glycoproteins with N-terminal $\Delta 32$ or $\Delta 83$ amino acid deletions. No E transcripts were noted. Both M glycoprotein and E protein are essential for efficient maturation and release (29, 30). Inevitably, the fatal phenotype likely resulted from both inefficient production and mutation of essential structural proteins such as E and M (31, 32). Excess truncated M glycoprotein may also establish a dominant-negative phenotype that further impedes assembly and release. Because the N protein functions as an enhancer of subgenomic transcription and genome replication and infectivity, limited N protein production would also function to suppress expression of subgenomic ORFs (33, 34). It is intriguing that noncanonical sites were most readily detected in chimeras containing the renetworked TRS-2-L site (CCGGAT) linked with WT TRS-B sites, because many fewer leader-containing transcripts were detected in chimeras with WT TRS-L (icSARS-CoV Rec1.3). Evolutionary pressure may have minimized the number of cryptic noncanonical TRS interactions located within the WT genome, pressures that were never applied to the icSARS-CoV CRG genome. Mapping noncanonical starts may allow for the efficient design of quiescent TRS sites in the icSARS CRG backbone that are calculated to express subgenomic mRNAs encoding N-terminal deletions in critical structural proteins, but only after recombination events with WT.

The strategy described herein provides a rational approach for minimizing viability of progeny RNA recombinant CoVs; however, double intragenic recombinants, especially within the ≈ 20 -kb SARS replicase ORF, would not be affected by the redesigned TRS circuitry. A fundamental theme in postgenomic research and systems biology will be to elucidate the complex interactions that regulate virus gene expression, polyprotein processing, transcription and replication, genome packaging, and assembly and release. In addition to the nidovirus TRS circuit paradigm, many positive-strand RNA viruses encode proteases that cleave large polyproteins at select sites. Remodeling protease cleavage site specificity might establish a genetic trap that is triggered by recombination events that scrambled different polyprotein processing networks (35, 36). Experimental phage evolution suggests an alternative approach (37, 38). Compensatory mutations occur when fitness loss caused by one mutation is remedied by its epistatic interactions with a second mutation in a different genome location. Often, compensatory mutations are extragenic and independently deleterious in the parent genome (38). Vaccine chassis that contain one or more sets of compensatory mutations will encode genetic traps that are triggered by recombination events that disrupt epistatic interactions. Complex interaction networks in genome encapsidation and virion formation might also be exploited in the design of recombination-resistant viruses as well (32, 39). Live virus vaccine platforms that encode new regulatory circuits provide a means toward enhancing safety and stabilizing attenuating mutations, especially against recombination repair.

Methods

Viruses and Cells. The Urbani and icSARS strains of SARS-CoV (AY278741), icSARS-CoV Luc, icSARS-CoV Luc1, icSARS-CoV Luc2, and the icSARS CRG and PRG recombinant viruses were propagated on Vero E6 cells as described in ref. 8. Cultures of Vero E6 cells were infected at a multiplicity of infection of 0.1

pfu for 1 h, and the samples were titered by plaque assay. All virus work was performed in a biological safety cabinet in a biosafety level 3 laboratory containing redundant exhaust fans as described in ref. 8.

Construction of *Renilla* Luciferase Encoding SARS-CoV Recombinant Clones. Plasmid DNA was amplified in One Shot Top 10 chemically competent cells (Invitrogen, Carlsbad, CA) and purified with the Qiaprep miniprep kit (Qiagen, Valencia, CA). DNA fragments were isolated from 1.0% agarose gels with the Qiaquick gel extraction kit (Qiagen) and visualized by using Dark Reader technology (Clare Chemical Research, Denver, CO). The six subgenomic cDNA clones (A–F) span the SARS-CoV genome (9). ORF 7a/b, located within SARS F (nt 27273–27772), was replaced with the *Renilla* luciferase gene as described with GFP in ref. 14.

To introduce mutations into the ORF7 TRS site, a forward primer (Ppum3: 5'-GCTGTGACATTAAGGACCTGC-CAAAAG-3') was used concurrently with reverse primers (3MUT3: 5'-AGGTGCACCTGCAGCCATTTTAATT-TATCCGGTTTATGGATA-3' or 2MUT3: 5'-AGGTGCACCTGCAGCCATTTTAATTTATCCGGTTTATGGATA-3'). Amplicon 1 (TRS-2) contained three mutations (CCGGAT), whereas amplicon 2 (TRS-1) had two mutations (ACGGAT) in the TRS site flanked by AarI and PpumI sites. A third amplicon (AMP3), flanked by AarI and PacI sites, was amplified with forward primer (3MUT5: 5'-GGTGCACCTGCAAATAAATGGCTTCCA-3') and reverse primer (PacI3: 5'-TAAAGTGAGCTCTTAATTAATTACTGCTCG-3'). After digestion, AMP1 and AMP2 were ligated separately to AMP3, and the 1.34-kb cDNA was cloned into pTOPO PCR-XL (Invitrogen). The mutated TRS sites were inserted into the icSARS WT luciferase (icSARS-CoV Luc) cDNA F construct and verified by sequence.

Construction of SARS Plasmids Containing Redesigned TRS Circuits. To create the TRS-L CCGGAT sequence, the SARS A plasmid was amplified with primer set M13R3 (5'-CAGGAAACAGCTATGAC-3') and MuL1– (5'-AAAATCCGGTTAGAGAACA-GATCTACAAGAG-3') or MuL1+ (5'-CTAACCGGATTTTAAATCTGTGTAGCTGTC-3') and SARS 453– (5'-ATAGGGCTGTTCAAGCTGGGG-3'). After overlapping PCR, the resulting ≈ 620 -bp product was cloned and sequenced. The insert was digested with MluI and AvrII and inserted into the SARS A plasmid. To mutate the spike (S) gene TRS, the SARS E fragment was PCR-amplified with primer sets SARS no. 37 (5'-TGCTGGCTCTGATAAAGGAG-3') and MuSgene– (5'-NNNCACCTGCACATATCCGGTTAGTTGTTAACAAGAATATCAC-3') or MuSgene+ (5'-NNNCACCTGCACACCGGATATGTT-TATTTCTTATTATTCTTACTCTC-3') and no. 10 AgeI– (5'-CATCAAGCGAAAAGGCATCAG-3'). These fragments were digested with restriction enzyme AarI, ligated, and subcloned. The mutated amplicon was digested with BsmBI and AgeI and inserted into the SARS E plasmid.

The SARS F plasmid containing the remaining TRS sites was PCR-amplified with the following primer sets: SARS no. 44 (5'-TGATCCTCTGCAACCTGAGC-3') and MuEgene– (5'-NNNCACCTGCATAAATCCGGACTACTTTCTTGTGCTTAC-3'); MuEgene+ (5'-NNNCACCTGCGTCCGGATTTATGTACTCATTCGTTTCGG-3') and MuMgene– (5'-NNNCACCTGCAATAGTTAATCCGGTTAGACCAGAAGAT-CAG-GAAC-3'); and MuMgene+ (5'-NNNCACCTGCGGATTAAC-TATTATT-ATTATTCTGTTTGG-3') and 28033– (5'-TACCAACACCTAGCTATAAGC-3'). The three amplicons were digested with AarI, directionally ligated, and subcloned. A clone containing the new consensus sequence CCGGAT for the E and M genes was digested with SmaI and NdeI and inserted into the SARS F plasmid (SARS F muE/M). The SARS N gene TRS was

constructed with MuGene1 (5'-GCTGCATTTAGAGACG-TACTTGTGTTTAAATAACCGGATAAAT-TAAAAT-GTCTGATAATGG-3') and SARS 3' Ng (5'-TTAATTAAT-TATGCCTGAGTTGAATCAGCAG-3'). The product was digested with BsmBI and inserted into plasmid SARS F muE/M (SARS F muE/M/N). To alter the ORF 3a TRS, amplicons were isolated with primer sets [SARS no. 44 and SARSX1- (5'-CGT-CTCATGTGTAATGTAATTTGACACCC-3') or SARSX1+ (5'-CGTCTCACA-CATAACCGGATTTATGGATTTGTT-TATGAGATTTTTTAC-3') and 28033-] and joined by ligation at the flanking BsmBI sites. This product was inserted into SARS F muE/M/N by using SmaI-NdeI sites (SARS F mu3a/E/M/N). Primer sets [SARS no. 47 (5'-GTGCTTGCTGTTGTCTACAG-3') and SARSX3- (5'-CGTCTCCGTCGG-GGATGTAGCCA-CAGTGATCTC-3'), SARSX3+ (5'-CGTCTCCGGACGCTT-TCTT-ATTACAAATTAGGAG-3') and SARSX4- (5'-CGT-CTCATATCCGGTTTATGGATAA-TCTAACCATCCATAG-3'), and SARSX4+ (5'-CGTCTCATATGAAAATTATTCTCT-TCTG-AC-3') and 28033-] were used to generate three PCR fragments that were digested with BsmBI, ligated with T4 DNA ligase, and subcloned. A clone containing only the required changes in TRS sites regulating subgenomic transcription of ORF6 and 7 was digested with AvrII and inserted into plasmid SARS Fmu 3a/E/M/N (SARS Fmu 3a/E/M/6/7/N). Finally, primer set SARS no. 48 (GGACTTTCAGGATTGCTATTTG) and SARSX5- (CGTCTCATCCGGT-TAGACTTTGGTACAAG-GTTC) and set SARSX5+ (CGTCTCCCGGATATGAAACT-TCTCATTTGTTTGGAC) and SARSX5 (NNNTAATTAAT-TAATTT-GTTCGTTTATTAAACAACA) created PCR products that were similarly joined by using BsmBI and T4 DNA ligase. This product was introduced into plasmid SARS Fmu 3a/E/M/6/7/N by using the NdeI-BstEII restriction sites. This final construct (SARS F CRG) was verified by sequence.

Isolation of Recombinant Viruses. The SARS full-length cDNA was assembled, and full-length transcripts were synthesized and

mixed with polyadenylated N gene transcripts and then electroporated into cells (9, 40). Viruses were plaque-purified in Vero E6 cells, and stock was grown in 75-cm² flasks.

Northern Blot Analysis. Intracellular RNA was isolated by using RiboPure reagents (Ambion, Austin, TX) at 12 h after infection. The mRNA was isolated by using Qiagen's Oligotex mRNA spin-column reagents, treated with glyoxal, and separated on agarose gels by using NorthernMax-Gly (Ambion). The RNA was transferred to BrightStar-Plus membrane (Ambion) for 4–5 h, cross-linked by UV light, prehybridized, and probed with an N gene-specific oligodeoxynucleotide probe (5'-cttgactgcgcg-ctctgct^bccct^bct^bgc^b-3'; biotinylated nucleotides are designated with a superscript "b"). Blots were hybridized overnight and washed with low- and high-stringency buffers, and the filters were incubated with alkaline phosphatase-conjugated streptavidin. The filters were incubated with the chemiluminescent substrate CDP-STAR, overlaid with film, and developed.

Western Blot Analysis. Twelve hours after infection, cells were washed in 1× PBS, lysed in buffer containing 20 mM Tris-HCl (pH 7.6), 150 mM NaCl, 0.5% deoxycholine, 1% Nonidet P-40, and 0.1% SDS, and postnuclear supernatants were added to an equal volume of 5 mM EDTA/0.9% SDS. Samples were then heat-inactivated for 30 min at 90°C, loaded onto 4–20% Criterion gradient gels (Bio-Rad, Hercules, CA), and transferred to PVDF membrane (Bio-Rad). Blots were probed with polyclonal mouse sera against the SARS-CoV ORF3a, S, or N proteins diluted 1:200 and developed by using ECL chemiluminescence reagents (GE Healthcare, Piscataway, NJ). *Renilla* luciferase expression was verified by using commercial antibodies (Chemicon International, Temecula, CA).

We thank the University of North Carolina Vaccine, Sequencing, and Oligonucleotide Centers. This work was supported by National Institutes of Health Grants AI23946-S1, AI059136, and AI059443 (to R.S.B.).

- Kew, O. M., Sutter, R. W., de Gourville, E. M., Dowdle, W. R. & Pallansch, M. A. (2005) *Annu. Rev. Microbiol.* **59**, 587–635.
- Seligman, S. J. & Gould, E. A. (2004) *Lancet* **363**, 2073–2075.
- Poon, L. L., Guan, Y., Nicholls, J. M., Yuen, K. Y. & Peiris, J. S. M. (2004) *Lancet Infect. Dis.* **4**, 663–671.
- Guan, Y., Zheng, B. J., He, Y. Q., Liu, X. L., Xhuan, Z. X., Cheung, C. L., Luo, S. W., Li, P. H., Zhang, L. J., Guan, Y. J., et al. (2003) *Science* **302**, 276–278.
- Li, W., Shi, Z., Yu, M., Ren, W., Smith, C., Epstein, J. H., Wang, H., Cramer, G., Hu, Z., Zhang, H., et al. (2005) *Science* **310**, 676–679.
- Wang, L., Junker, D. & Collisson, E. W. (1993) *Virology* **192**, 710–716.
- Rota, P. A., Oberste, M. S., Monroe, S. S., Nix, W. A., Campagnoli, R., Icenogle, J. P., Penaranda, S., Bankamp, B., Maher, K., Chen, M. H., et al. (2003) *Science* **300**, 1394–1399.
- Yount, B., Roberts, R. S., Sims, A. C., Deming, D., Frieman, M. B., Sparks, J., Denison, M. R., Davis, N. & Baric, R. S. (2005) *J. Virol.* **79**, 14909–14922.
- Yount, B., Curtis, K., Fritz, E., Hensley, L., Jahrling, P., Prentice, E., Denison, M., Geisbert, T. & Baric, R. (2003) *Proc. Natl. Acad. Sci. USA* **100**, 12995–13000.
- Sawicki, S. G. & Sawicki, D. L. (1990) *J. Virol.* **64**, 1050–1056.
- Schaad, M. C. & Baric, R. S. (1994) *J. Virol.* **68**, 8169–8179.
- Zuniga, S., Sola, I., Alonso, S. & Enjuanes, L. (2004) *J. Virol.* **78**, 980–994.
- Sola, I., Moreno, J. L., Zuniga, S., Alonso, S. & Enjuanes, L. (2005) *J. Virol.* **79**, 2506–2516.
- Sims, A. C., Baric, R. S., Yount, B., Burkett, S. E., Collins, P. L. & Pickles, R. J. (2005) *J. Virol.* **79**, 15511–15524.
- Keck, J. G., Soe, L. H., Makino, S., Stohlman, S. A. & Lai, M. M. (1988) *J. Virol.* **62**, 1989–1998.
- Smati, R., Silim, A., Guertin, C., Henrichon, M., Marandi, M., Arella, M. & Merzouki, A. (2002) *Virus Genes* **25**, 85–93.
- Thiry, E., Meurens, F., Muykens, B., McVoy, M., Gogev, S., Thiry, J., Vanderplasschen, A., Epstein, A., Keil, G. & Schynts, F. (2005) *Rev. Med. Virol.* **15**, 89–103.
- Cheng, C.-P., Serviene, E. & Nagy, P. D. (2006) *J. Virol.* **80**, 2631–2640.
- Figlerowicz, M., Nagy, P. D. & Bujarski, J. J. (1997) *Proc. Natl. Acad. Sci. USA* **94**, 2073–2078.
- Nagy, P. D., Pogany, J. & Simon, A. E. (1999) *EMBO J.* **18**, 5653–5665.
- Nagy, P. D. & Simon, A. E. (1997) *Virology* **235**, 1–9.
- Goebel, S. J., Taylor, J. & Masters, P. S. (2004) *J. Virol.* **78**, 7846–7851.
- Martin, D. P., van der Walt, E., Posada, D. & Rybicki, E. P. (2005) *PLoS Genet.* **4**, 475–479.
- Goebel, S. J., Taylor, J. & Masters, P. S. (2004) *J. Virol.* **78**, 669–682.
- Atsumi, S. & Little, J. W. (2004) *Genes Dev.* **18**, 5621–5629.
- Atsumi, S. & Little, J. W. (2006) *Proc. Natl. Acad. Sci. USA* **103**, 4558–4563.
- Endy, D., You, L., Yin, J. & Molineux, I. J. (2000) *Proc. Natl. Acad. Sci. USA* **97**, 5375–5380.
- Wertz, G., Perepelitsa, V. P. & Ball, L. A. (1998) *Proc. Natl. Acad. Sci. USA* **95**, 3501–3506.
- Curtis, K. M., Yount, B. & Baric, R. S. (2002) *J. Virol.* **76**, 1422–1434.
- Kuo, L. & Masters, P. S. (2003) *J. Virol.* **77**, 4597–4608.
- deHaan, C. A. M., Kuo, L., Masters, P. S., Vennema, H. & Rottier, P. J. (1998) *J. Virol.* **72**, 6838–6850.
- Vennema, H., Godeke, G. J., Rossen, J. W., Voorhout, W. F., Horzinek, M. C., Opstelten, D. J. & Rottier, P. J. (1996) *EMBO J.* **15**, 2020–2028.
- Almazan, F., Galan, C. & Enjuanes, L. (2004) *J. Virol.* **78**, 12683–12688.
- Yount, B., Curtis, C. & Baric, R. S. (2000) *J. Virol.* **74**, 10600–10611.
- Denison, M. R., Yount, B., Brockway, S. M., Graham, R. L., Sims, A. C., Lu, X. & Baric, R. S. (2004) *J. Virol.* **78**, 5957–5965.
- Snijder, E. J., Bredenbeek, P. J., Dobe, J. C., Thiel, V., Ziebuhr, J., Poon, L. L., Guan, Y., Rozanov, M., Spaan, W. J. & Gorbalenya, A. E. (2003) *J. Mol. Biol.* **331**, 991–1004.
- Bacher, J. M., Bull, J. & Ellington, A. D. (2003) *BMC Evol. Biol.* **3**, 24–35.
- Poon, A. & Chao, L. (2005) *Genetics* **170**, 989–999.
- Escors, D., Izeta, A., Capiscol, C. & Enjuanes, L. (2003) *J. Virol.* **77**, 7890–7902.
- Yount, B., Denison, M. R., Weiss, S. R. & Baric, R. S. (2002) *J. Virol.* **76**, 11065–11078.